IMMUNOLOGY

The costimulatory molecule CD226 signals through VAV1 to amplify TCR signals and promote IL-17 production by CD4$^+$ T cells

Guillaume Gaud[1], Romain Roncagalli[2], Karima Chaoui[3], Isabelle Bernard[1], Julien Familiades[1], Céline Colacios[1], Sahar Kassem[1], Bernard Monsarrat[3], Odile Burlet-Schiltz[3], Anne Gonzalez de Peredo[3], Bernard Malissen[2,4]*, Abdelhadi Saoudi[1]*†

The activation of T cells requires the guanine nucleotide exchange factor VAV1. Using mice in which a tag for affinity purification was attached to endogenous VAV1 molecules, we analyzed by quantitative mass spectrometry the signaling complex that assembles around activated VAV1. Fifty VAV1-binding partners were identified, most of which had not been previously reported to participate in VAV1 signaling. Among these was CD226, a costimulatory molecule of immune cells. Engagement of CD226 induced the tyrosine phosphorylation of VAV1 and synergized with T cell receptor (TCR) signals to specifically enhance the production of interleukin-17 (IL-17) by primary human CD4$^+$ T cells. Moreover, co-engagement of the TCR and a risk variant of CD226 that is associated with autoimmunity (rs763361) further enhanced VAV1 activation and IL-17 production. Thus, our study reveals that a VAV1-based, synergistic cross-talk exists between the TCR and CD226 during both physiological and pathological T cell responses and provides a rational basis for targeting CD226 for the management of autoimmune diseases.

INTRODUCTION

VAV1, a guanine nucleotide exchange factor (GEF) for Rho family guanosine triphosphatases (GTPases), is exclusively expressed in hematopoietic cells and plays a crucial role in T cell receptor (TCR) signaling (*1*, *2*). After TCR engagement by antigen, VAV1 is recruited to the transmembrane adaptor protein LAT (linker for activation of T cells) through the adaptors GADS (Grb2-related adaptor downstream of Shc) and SLP76 (SH2 domain containing leukocyte protein of 76 kDa), leading to the phosphorylation of VAV1's acidic domain by LCK (lymphocyte-specific protein tyrosine kinase). Although VAV1 acts primarily as a GEF, its scaffolding role is also important for T cell activation (*3*, *4*). The functional importance of VAV1, in both developing and mature T cells, has been highlighted by several studies showing that VAV1-deficient mice exhibit a strong impairment in thymic selection and contain mature T cells that display reduced proliferation, activation, and cytokine production (*5*). This phenotype results from a decrease in TCR-induced signaling events that involve Ca^{2+} mobilization, as well as activation of the extracellular signal–regulated kinase (ERK) family of mitogen-activated protein kinases, phosphoinositide 3-kinase (PI3K), the serine-threonine kinase AKT, and transcription factors such as nuclear factor of activated T cells and nuclear factor κB (NF-κB) (*1*, *6*–*8*).

In addition to its role in TCR signaling, some studies have reported a role for VAV1 in conveying signals from cytokine receptors and costimulatory molecules in T cells. For example, VAV1 plays a role in the synergic signals induced by the TCR and the costimulatory molecule CD28 (*9*). Most of the studies concerning the role of VAV1 in T cell activation have been performed using transformed cell lines and hypothesis-driven approaches, which do not allow for a global analysis of VAV1 interactors. Consequently, the composition of the VAV1 signalosome in primary T cells, the involvement of VAV1 in signaling pathways downstream of costimulatory molecules, and their integration with TCR signaling remain open questions.

Here, we combined mouse genetics and quantitative proteomics to characterize the VAV1 interactome in primary CD4$^+$ T cells in a comprehensive and time-resolved manner. Among the identified partners of VAV1, the costimulatory molecule CD226 [also called DNAM-1 (DNAX accessory molecule–1)] was one of the most highly enriched VAV1 interactors at early time points after T cell activation. Functional analyses showed that CD226 engagement triggered VAV1 activation through tyrosine phosphorylation and synergized with signaling through TCR to positively regulate cytokine production by CD4$^+$ T cells. CD226 signaled through VAV1 to specifically amplify TCR-mediated ERK signals and selectively promote interleukin-17 (IL-17) production by human primary CD4$^+$ T cells. In CD4$^+$ T cells harboring the CD226 rs763361 risk variant associated with autoimmune diseases (*10*, *11*), co-engagement of TCR and CD226, but not of TCR alone, enhanced ERK and VAV1 activation compared to co-engagement of TCR and wild-type CD226, resulting in increased IL-17 production. This highlights the physiopathological importance of the VAV1-dependent synergic cross-talk between TCR and CD226 identified in the present study.

RESULTS

VAV1 can be specifically affinity-purified from CD4$^+$ T cells of Vav1^{OST} mice

To study the composition and dynamics of the VAV1 signalosome in primary CD4$^+$ T cells, we generated knock-in mice expressing VAV1 with a OneStrepTag (OST) (*12*) fused to the C terminus, called *Vav1*^{OST} here and also known as B6-*Vav1*^{tm1Mal} (fig. S1). Flow

[1]Centre de Physiopathologie de Toulouse Purpan, Université de Toulouse, CNRS, Inserm, Toulouse 31300, France. [2]Centre d'Immunologie de Marseille-Luminy, Aix-Marseille Université, Inserm, CNRS, 13288 Marseille, France. [3]Institut de Pharmacologie et de Biologie Structurale, Université de Toulouse, CNRS UMR 5089, 31077 Toulouse Cedex, France. [4]Centre d'Immunophénomique, Aix-Marseille Université, Inserm, CNRS, 13288 Marseille, France.
*These authors contributed equally to this work.
†Corresponding author. Email: abdelhadi.saoudi@inserm.fr

cytometry analysis of mice homozygous for the *Vav1*^{OST} allele showed no change in thymocyte or peripheral subsets of T cells when compared to wild-type mice (Fig. 1, A to C). The addition of the OST had no effect on the abundance and phosphorylation status of VAV1 or on Ca^{2+} mobilization in $CD4^+$ T cells (Fig. 1, D and E). Comparison of $CD4^+$ T cells isolated from wild-type and *Vav1*^{OST} mice and stimulated in vitro with pervanadate, a compound that activates T cells by inhibiting protein tyrosine phosphatases, demonstrated that the OST sequence had no measurable effect on the global pattern of tyrosine phosphorylation (Fig. 1F). VAV1 baits affinity-purified from $CD4^+$ T cell lysates were subjected to immunoblot analysis using antibodies recognizing phosphotyrosine and VAV1. Phosphorylated VAV1 and other phosphorylated proteins associated with VAV1 were specifically detected in affinity-purified samples from *Vav1*^{OST} $CD4^+$ T cells, whereas no phosphorylation signals were detected after affinity purification was performed on wild-type $CD4^+$ T cells (Fig. 1G). Phospholipase C–γ (PLC-γ), LAT, and growth factor receptor–bound protein 2 (GRB2), all of which are known partners of VAV1 (*13*–*15*), were readily detected in the affinity-purified VAV1^{OST} complexes after stimulation of $CD4^+$ T cells with pervanadate (Fig. 1H). Therefore, $CD4^+$ T cells from *Vav1*^{OST} mice are amenable to analysis by affinity purification coupled to mass spectrometry (AP-MS).

Analysis of the VAV1 interactome in primary $CD4^+$ T cells identifies diverse VAV1-binding partners

Primary $CD4^+$ T cells from wild-type and *Vav1*^{OST} mice were stimulated with pervanadate for 0, 30, 120, or 300 s, and protein complexes containing VAV1^{OST} baits were isolated and analyzed by liquid chromatography coupled to tandem MS (LC-MS/MS), as previously described (*16*). Global analysis of MS intensities showed reliable reproducibility between each condition and between biological replicates (fig. S2, A to C). Proteins that displayed enrichment greater than five-fold and a $P < 0.05$ were selected, leading to the identification of 50 high-confidence interacting partners of VAV1 (Fig. 2, A and B, and table S1). These 50 proteins included many functional classes, such

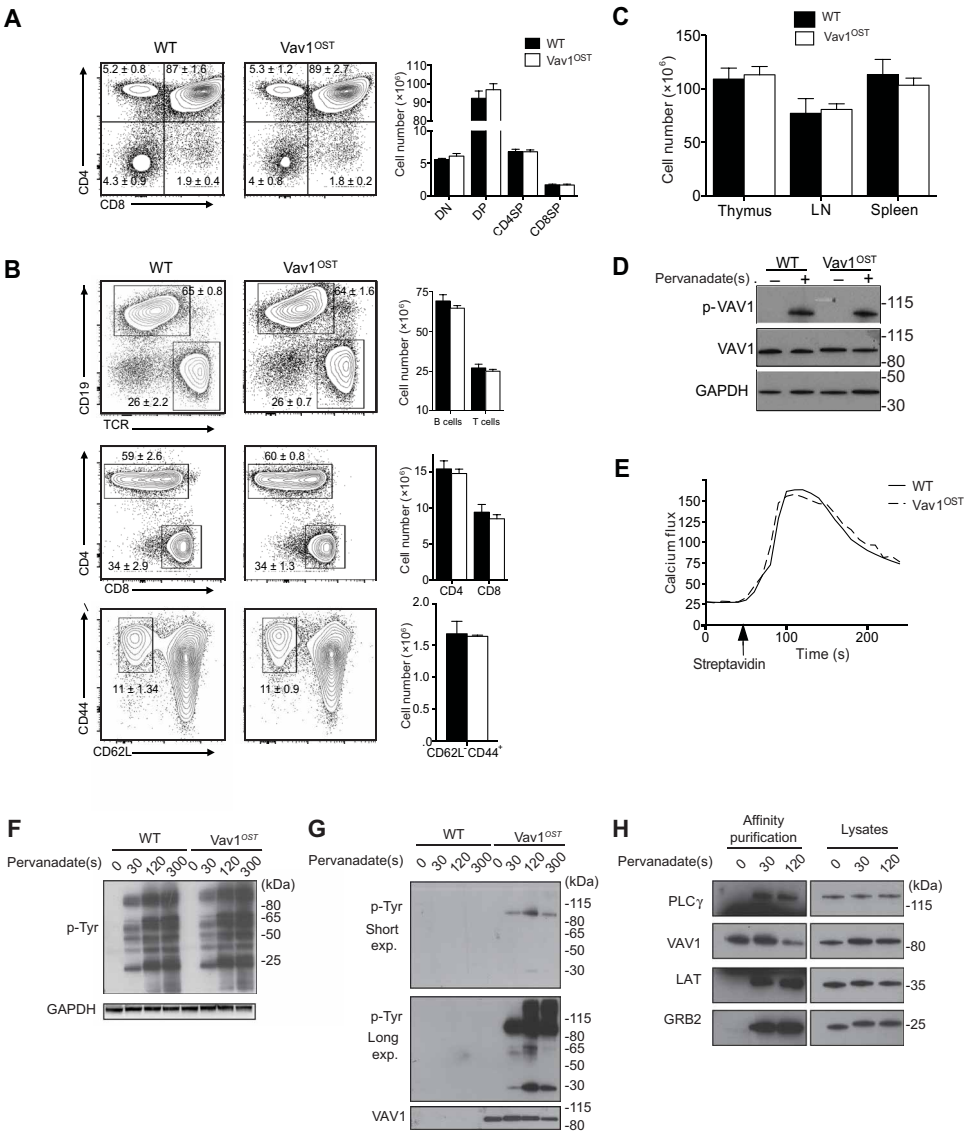

Fig. 1. Normal T cell development and functions in *Vav1*^{OST} mice. (**A**) Representative flow cytometry analysis of thymocytes from wild-type (WT) and *Vav1*^{OST} mice. Graphs represent total numbers of thymocyte subsets. (**B**) Representative flow cytometry analysis of cells from spleens of WT and *Vav1*^{OST} mice. Graphs represent total numbers of lymphocyte subsets. (**C**) Cellularity of thymus, lymph nodes (LN), and spleen from WT and *Vav1*^{OST} mice. In (A) to (C), data are presented as means ± SD (n = 5 mice per group). (**D**) Immunoblot showing the abundance of VAV1 and phosphorylated VAV1 (p-VAV1) before and after pervanadate activation of $CD4^+$ T cells from WT and *Vav1*^{OST} mice. Glyceraldehyde-3-phosphate dehydrogenase (GAPDH) is a loading control. Data are representative of three independent experiments. (**E**) Changes in intracellular Ca^{2+} in WT and *Vav1*^{OST} $CD4^+$ T cells stimulated with a biotinylated monoclonal antibody recognizing CD3 and treated with streptavidin to cross-link and activate CD3. The arrow indicates the addition of streptavidin. Results are representative of two independent experiments. (**F**) Immunoblot showing phosphorylated tyrosine (p-Tyr) in equal amounts of total lysates of $CD4^+$ T cells harvested from WT and *Vav1*^{OST} mice and stimulated with pervanadate for the indicated durations. GAPDH is a loading control. Results are representative of five independent experiments. (**G**) Immunoblots showing p-Try in equal amounts of OST affinity–purified lysates from WT and *Vav1*^{OST} $CD4^+$ T cells stimulated with pervanadate for the indicated durations. VAV1 is a loading control. Both short and long exposures of the blot are shown. Results are representative of three independent experiments. (**H**) Immunoblot showing PLC-γ, VAV1, LAT, and GRB2 in equal amounts of whole-cell lysates and lysates that were subjected to OST affinity purification from WT and *Vav1*^{OST} $CD4^+$ T cells stimulated with pervanadate for the indicated durations. Results are representative of three independent experiments. Numbers to the right of the blot correspond to the molecular size in kilodaltons.

as tyrosine and serine-threonine kinases (18%), adaptors (22%), and protein phosphatases (12%), as well as three GTPase-activating proteins (GAPs): RHG30 (RHO GAP 30), GMIP (GEM-interacting protein), and ACAP1 (ArfGAP with coiled-coil, ankyrin repeat, and pleckstrin homology domain 1) (Fig. 2B and fig. S3, A to C). As expected, we detected several known partners of VAV1 that cooperate in the assembly of the TCR signalosome, including the tyrosine kinases LCK, the proto-oncogene tyrosine-protein kinase FYN, and the ζ-chain–associated protein kinase 70 (ZAP70). By phosphorylating the adaptor LAT and SLP76, these kinases lead to the recruitment of VAV1 through NCK (noncytosolic region of tyrosine kinase adaptor protein) (*17*) or the transmembrane receptor CD6 (*16*, *18*) and to the activation of VAV1 through tyrosine phosphorylation (*19*–*21*). Consistent with these findings, LAT, SLP76, NCK, and CD6 were enriched in the VAV1 interactome. Proteins involved in transducing VAV1-mediated signaling were also present, as illustrated by the tyrosine kinase ITK (IL-2–inducible T cell kinase), the phospholipase PLC-γ1, and the p85 subunit of PI3K (*8*, *22*). We also identified CBLB (Cbl proto-oncogene B), an E3 ubiquitin ligase that attenuates VAV1-dependent CD28 signaling (*6*), as well as GRB2, THEMIS (thymocyte-expressed molecule involved in selection), and PTPN6 (tyrosine-protein phosphatase nonreceptor 6), which form a complex that directly or indirectly associates with VAV1 (*23*, *24*).

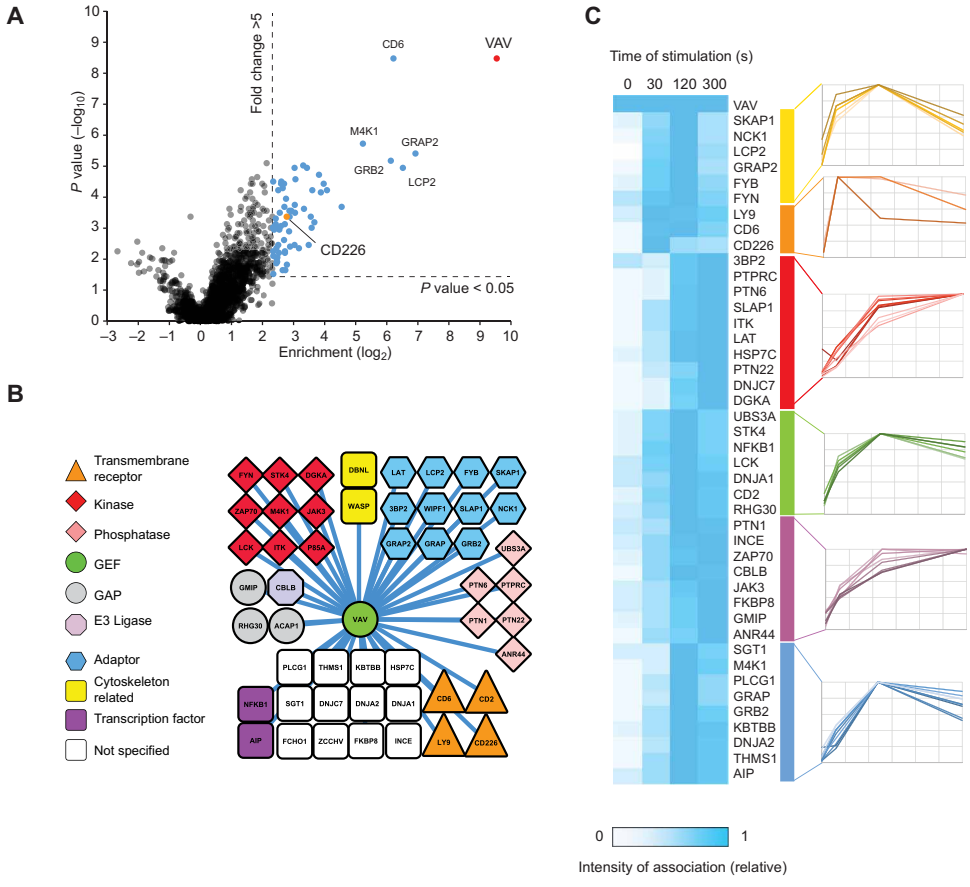

Fig. 2. Analysis of the VAV1 interactome in primary *Vav1*^{OST} CD4$^+$ T cells. (**A**) Volcano plot of proteins identified as interacting with VAV1 by AP-MS. The mean *P* value is plotted against the corresponding mean fold change for *Vav1*^{OST} versus WT samples (enrichment). Proteins were classified as VAV1 interactors (blue) if they displayed enrichment greater than fivefold and $P < 0.05$. Subsequently, *P* values were corrected using the Benjamini-Hochberg (BH) method to determine the final VAV1 interactome. The VAV1 bait is shown in red, and dashed lines represent thresholds on *P* value and enrichment to identify specific VAV1 interactors. CD226 is highlighted in orange. (**B**) Each protein interacting with the Vav1^{OST} bait is represented as a node linked by an edge to the Vav1^{OST} bait. Proteins are identified by their UniProtKB designation and color-coded according to their function or protein family. (**C**) Label-free quantitative analysis of the kinetics of the binding of various proteins to VAV1 in mouse CD4$^+$ T cells that were either unstimulated or stimulated for 30, 120, or 300 s with pervanadate. The intensity of the association is shown from minimum (0) to maximum (1). Interacting proteins were clustered using Euclidean distance correlation on the basis of the similarities in their VAV1-binding kinetics.

Among the VAV1 interactors, a substantial number participate in cytoskeletal rearrangement and T lymphocyte motility. In particular, we identified the WASP (Wiskott-Aldrich syndrome protein) and WIPF1 (WAS/WASL-interacting protein family member 1), which form a complex that promotes TCR-dependent actin polymerization and causes immunodeficiencies when mutated (*25*). We also observed the presence of hematopoietic progenitor kinase 1 (HPK1) and Debrin-like protein [DBNL, also known as HPK1-interacting protein of 55 kDa (HIP-55)], both of which have been shown to form a complex that attenuates TCR signaling (*26*). In addition, the VAV1 interactome contained molecules required for receptor internalization and endocytosis, such as the adaptor the Src-like-adapter protein 1 (SLAP1) and F-BAR domain–only protein 1 (FCHO1) (*27*, *28*).

Using label-free quantification, we monitored the kinetics of the binding of interacting partners to VAV1 over four time points of stimulation by pervanadate, allowing us to cluster VAV1 interactors based on their kinetic profiles of recruitment to the bait (Fig. 2C and figs. S2C and S3C). A small cluster (orange in Fig. 2C) composed of the transmembrane receptors Ly9, CD6, and CD226 corresponded to proteins that were recruited within 30 s of T cell activation by pervanadate treatment. Three larger clusters (yellow, green, and blue in Fig. 2C) were composed of interactors that bound to VAV1 between 30 s and 2 min and were released after 2 min of pervanadate treatment. These clusters included kinases and adaptor proteins involved in signal initiation and propagation [SLP76/lymphocyte cytosolic protein 2 (LCP2), GRB2-related adapter protein 2 (GRAP2), FYN binding protein (FYB), FYN, PLC-γ, GRAP, GRB2, and mitogen-activated protein kinase kinase kinase kinase 1 (MAP4K1)]. The two remaining clusters (purple and red in Fig. 2C) were mainly composed of protein tyrosine phosphatases that terminate TCR signaling or are likely involved in the duration and rate of the TCR responses [protein tyrosine phosphatase, receptor type, C (PTPRC), PTN22, PTN1, and PTN6].

VAV1 is involved in CD226 signaling

CD226, also known as DNAM-1, is a transmembrane receptor present on natural killer (NK) cells, $CD8^+$ and $CD4^+$ T cells, and several types of myeloid cells. At early time points of T cell activation by pervanadate, the costimulatory molecule CD226 was one of the most highly enriched VAV1 interactors (Fig. 2A and fig. S3C), suggesting that VAV1 might play a role in CD226 signaling in T cells. To test this hypothesis, we first investigated the ability of CD226 to trigger intracellular signaling upon cross-linking with a monoclonal antibody that binds to CD226, using a human Jurkat cell line that overexpresses CD226 (J.CD226) (*29*), compared to wild-type Jurkat cells (J.Ctl) (Fig. 3A). Stimulation of both types of Jurkat cells by CD226 cross-linking increased the global quantities of tyrosine phosphorylation, reaching a peak 2 min after CD226 engagement (Fig. 3B). This effect was, however, more pronounced in J.CD226 cells than in J.Ctl cells. The engagement of CD226 led to the activation of VAV1, as shown by its phosphorylation on Tyr^{174} (Fig. 3, B and C). Using co-immunoprecipitation, we showed that CD226 interacted with VAV1 in J.CD226 cells soon after CD226 engagement, whereas CD226 did not interact with VAV1 at steady state (Fig. 3D). We confirmed the occurrence of a CD226-VAV1 interaction after engaging CD226 on primary human $CD4^+$ T cells by co-immunoprecipitation of CD226 with phosphorylated VAV1 molecules (Fig. 3E). CD226 ligation also led to ERK activation in J.CD226 cells (Fig. 3C), and this activation was strongly reduced after VAV1 knockdown (Fig. 3F), highlighting the importance of VAV1 in CD226-driven ERK signaling.

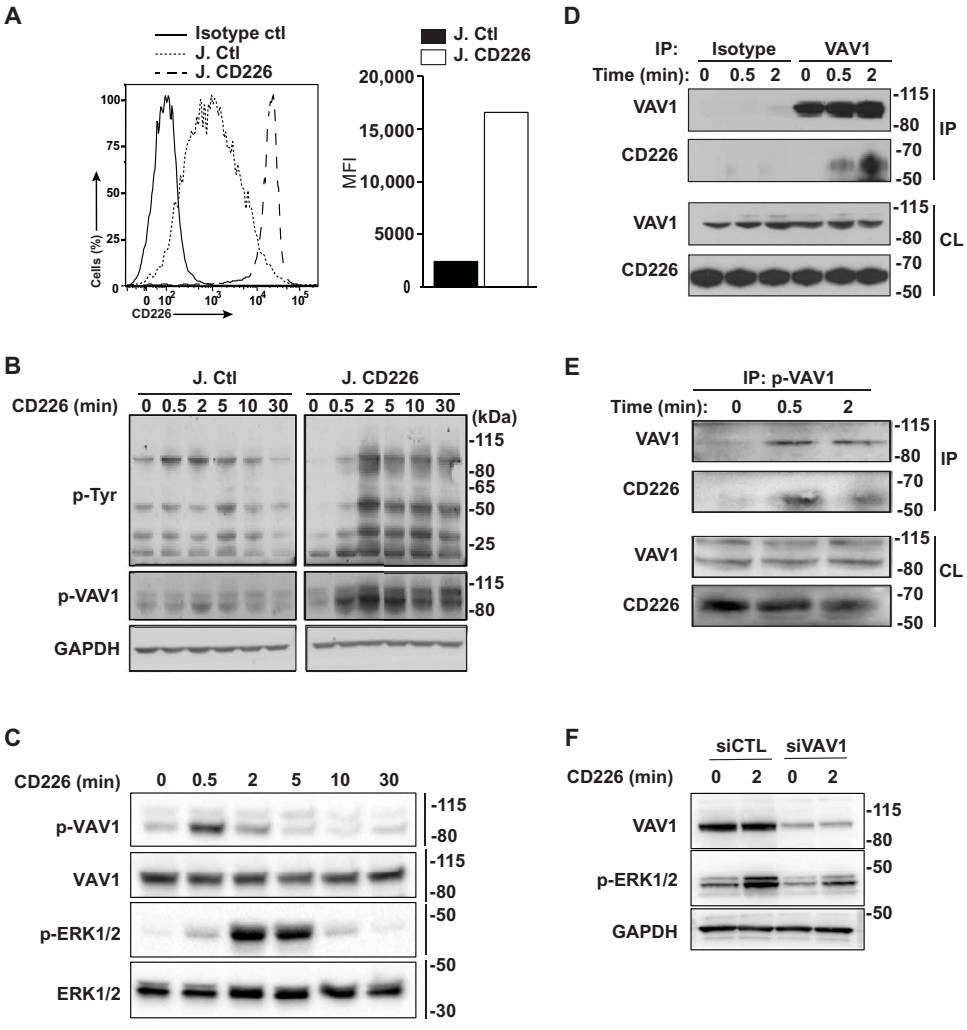

Fig. 3. VAV1 is part of the CD226 signaling pathway in T cells. (**A**) Representative flow cytometry histogram of CD226 surface abundance in control Jurkat cells (J.Ctl) and Jurkat cells overexpressing CD226 (J.CD226) and a graph showing the mean fluorescence intensities (MFI) of CD226 in J.Ctl and J.CD226 cells. Data are representative of five independent experiments. (**B**) Immunoblot showing p-Tyr and VAV1 phosphorylated on Tyr^{174} (p-VAV1) in equal amounts of total lysates from J.Ctl and J.CD226 cells that were either unstimulated or stimulated with the antibody that cross-links CD226 molecules for the indicated durations. GAPDH is a loading control. Results are representative of three independent experiments. (**C**) Immunoblot showing p-VAV1, p-ERK1/2, and total ERK1/2 (ERK1/2) in Jurkat cells treated as in (B). Results are representative of three independent experiments (**D**) Immunoblot analysis of J.CD226 cells left unstimulated or stimulated with the antibody that cross-links CD226 molecules for the indicated times followed by immunoprecipitation of VAV1 and analysis of immunoprecipitates (IP) and crude lysates (CL) with antibody directed against VAV1 or CD226. Results are representative of three independent experiments (**E**) Immunoblot analysis of primary human $CD4^+$ T cells left unstimulated or stimulated with the CD226 cross-linking antibody for the indicated times followed by immunoprecipitation of p-VAV1 and analysis of IP and CL with antibody directed against VAV1 or CD226. Results are representative of two independent experiments. (**F**) Immunoblot analysis of equal amounts of total lysates from J.CD226 cells expressing scrambled small interfering RNA (siRNA; siCTL) or siRNA directed against VAV1 mRNA (siVAV1). Cells were unstimulated or stimulated with the CD226 cross-linking antibody for 2 min. Blots were probed antibodies to VAV1, p-ERK1/2, and the loading control GAPDH. Results are representative of three independent experiments.

CD226 signals through VAV1 to synergize with the TCR and stimulate IL-17 production

Because CD226 signaling has not been reported to synergize with TCR signaling, we tested for this interaction by stimulating Jurkat cells with increasing amounts of an antibody that cross-links the CD3 subunits of the TCR, thereby stimulating TCR signaling, in the presence of increasing concentrations of either the antibody that cross-links CD226 molecules or a control antibody of the same isotype. When Jurkat cells were stimulated with a suboptimal dose of antibody that cross-links the CD3 molecules, co-engagement of CD226 led to a strong synergistic signal, as shown by the increased phosphorylation of VAV1 Tyr^{174} and of phosphorylated ERK1/2 (Fig. 4A). We further assessed whether VAV1 played a role in the ability of CD226 to synergize with CD3 during activation of ERK1/2. CD3 and CD226 engagement readily synergized after 2 and 5 min of stimulation in both Jurkat and primary human $CD4^+$ T cells, and this synergetic effect was dampened when VAV1 was knocked down (Fig. 4, B and C). Although AKT activation was increased after

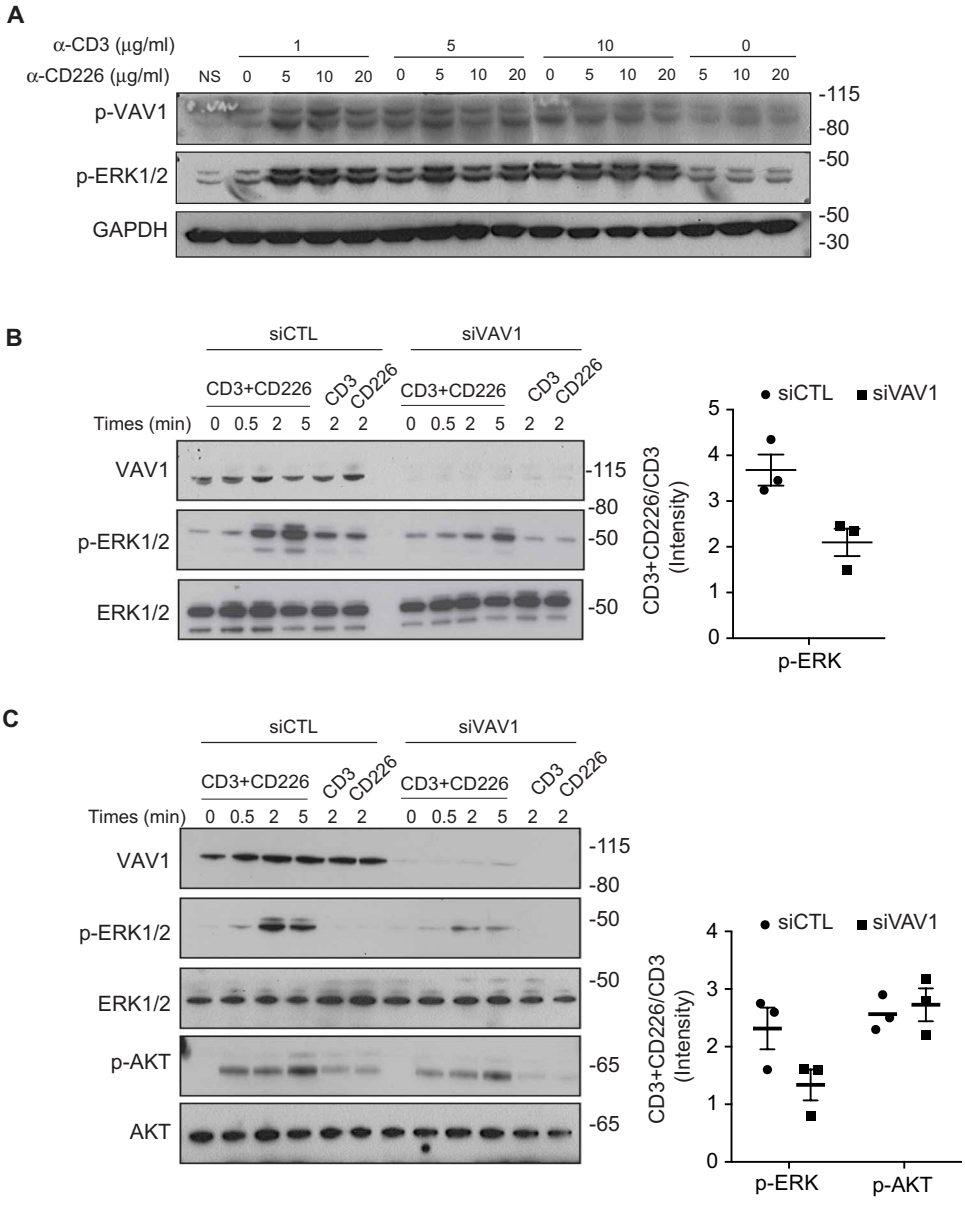

Fig. 4. VAV1 knockdown reduces the synergistic activity of CD3 and CD226 costimulation in T cells. (**A**) Immunoblot showing p-VAV1 and p-ERK1/2 in equal amounts of total lysates of J.CD226 cells that were unstimulated or stimulated with increasing amounts of an antibody that cross-links CD3 molecules associated with either a control antibody or an antibody that cross-links CD226 molecules for 2 min. GAPDH is a loading control. Results are representative of three independent experiments. (**B**) Immunoblot showing p-VAV1, p-ERK1/2, and total ERK1/2 in equal amounts of total lysates of J.CD226 cells expressing scrambled siRNA (siCTL) or siRNA directed against VAV1 mRNA (siVAV1). Cells were unstimulated, costimulated with antibodies that cross-link the CD226 and CD3 molecules (CD3+CD226), or stimulated with an antibody that cross-links either the CD3 (CD3) or the CD226 (CD226) molecules only for the indicated times, and lysates were probed with antibodies recognizing VAV1, p-ERK1/2, or total ERK1/2. The graph shows the relative abundances of p-ERK1/2, determined as a ratio of intensity of CD3+CD226 costimulation to that of CD3 stimulation alone at 2 min. Data are from three independent experiments. (**C**) Immunoblot analysis of equal amounts of proteins from total lysates of primary human $CD4^+$ T cells expressing siCTL or siVAV1. Cells were treated as in (B), and lysates were immunoblotted to show VAV1, p-ERK1/2, total ERK1/2, phosphorylated AKT (p-AKT), and total AKT. The graph shows the relative abundances of p-ERK1/2 and p-AKT, determined as a ratio of intensity of CD3+CD226 costimulation to that of CD3 stimulation alone at 2 min. Data are from three independent experiments.

co-engagement of CD3 and CD226, it was not affected by VAV1 knockdown, suggesting that VAV1 is crucial for some, but not all, CD226-driven signaling events.

To explore whether CD226 ligation was capable of potentiating TCR-driven cytokine production, we stimulated primary human $CD4^+$ T cells either with antibodies recognizing CD3 and CD226 or only with antibodies recognizing CD3 for 3 days. The secretion of IL-5, IL-10, IL-13, IL-17, granulocyte-macrophage colony-stimulating factor (GM-CSF), and interferon-γ (IFN-γ) was higher after CD226 and CD3 co-engagement compared to CD3 stimulation alone (Fig. 5A). We then investigated the importance of VAV1 for cytokine production driven by co-engagement of CD3 and CD226 using primary human $CD4^+$ T cells in which VAV1 had been knocked down. Given that knockdown of VAV1 reduced cytokine production upon engagement of CD3 alone, we presented the data as the ratio of cytokine secretion triggered by CD3 and CD226 co-engagement to that triggered by CD3 stimulation alone to emphasize the response specifically due to CD226 costimulation. Knocking down VAV1 had no major effect on IL-10, IL-5, IL-13, GM-CSF, or IFN-γ secretion but strongly reduced IL-17 secretion (Fig. 5B). Our results demonstrate a synergetic effect of CD3 and CD226 signaling on cytokine production by primary human $CD4^+$ T cells and highlight the role of VAV1 in CD226-driven production of IL-17.

The CD226 G307S risk variant favors IL-17 production and VAV1 activation

A nonsynonymous single-nucleotide polymorphism (SNP) resulting in an amino acid substitution (G307S) in the intracellular signaling domain of CD226 has been associated with several autoimmune inflammatory diseases including multiple sclerosis and type 1 diabetes (*10*, *11*). We analyzed whether CD226 engagement on $CD4^+$ T cells harboring this risk allele would increase the production of proinflammatory cytokines. We were particularly interested in the potential effect on IL-17 production given our observation that VAV1 is required for IL-17 secretion driven by CD226-CD3 co-engagement and because IL-17 is involved in the pathogenesis of multiple sclerosis and type 1 diabetes. In contrast

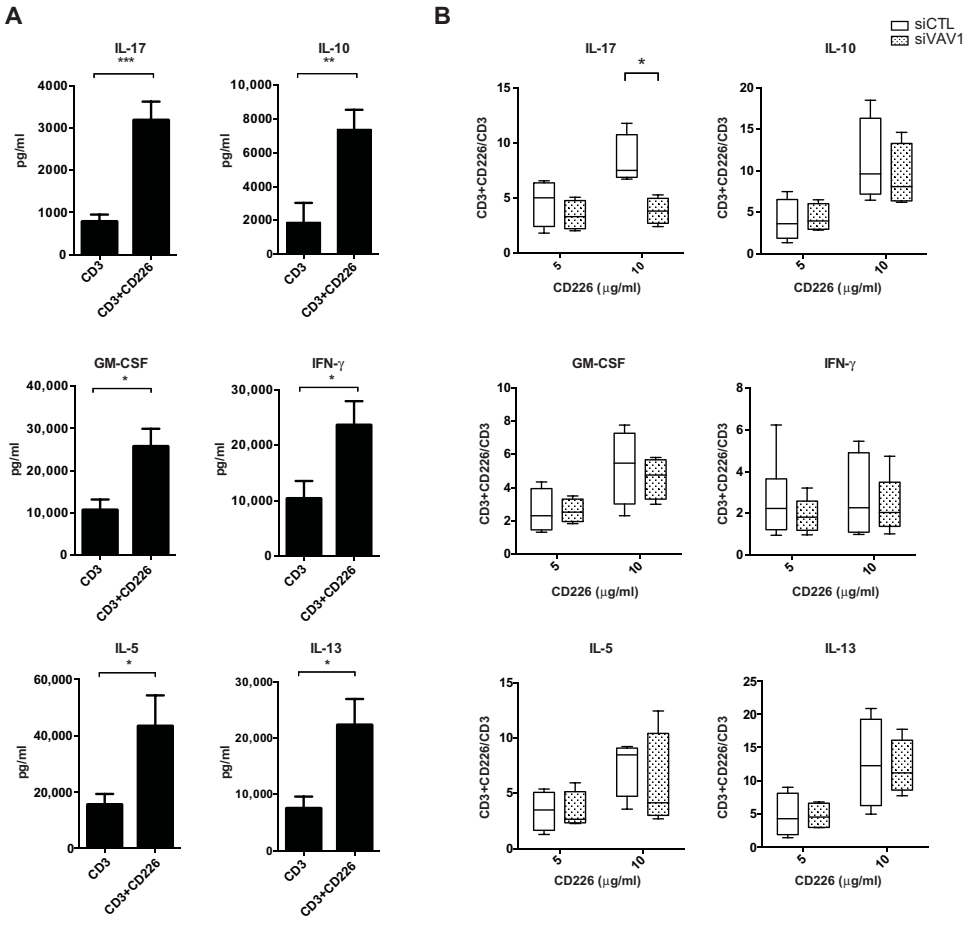

Fig. 5. VAV1 controls CD226-induced IL-17 secretion. (**A**) Secretion of IL-17, IL-10, GM-CSF, IFN-γ, IL-5, and IL-13 was quantified in supernatants of primary human CD4$^+$ T cells stimulated with CD3 antibody + immunoglobulin G1 (IgG1) isotype control (CD3) or CD3 and CD226 (CD3+CD226) antibodies for 3 days using cytometric beads array assay and expressed as picograms per milliliter. (**B**) Secretion of IL-17, IL-10, GM-CSF, IFN-γ, IL-5, and IL-13 was quantified in supernatants of primary human CD4$^+$ T cells expressing scrambled siRNA (siCTL) or siRNA directed against VAV1 mRNA (siVAV1) and stimulated with CD3 antibody + IgG1 isotype control (CD3) or CD3 and CD226 (CD3+CD226) antibodies for 3 days. The data are represented as ratio of cytokine production between CD3+CD226 and CD3 stimulations. All data are from eight unrelated donors. *$P \leq 0.05$, **$P \leq 0.01$, ***$P \leq 0.001$.

to naïve CD4$^+$CD45RA$^+$ T cells (fig S4, A to C), the co-engagement of CD226 and CD3 on effector CD4$^+$CD45RA$^-$ T cells increased IFN-γ, GM-CSF, and IL-10 production regardless of the CD226 allele (Fig. 6A). CD3 stimulation alone did not cause any difference in IL-17 secretion between cells carrying the protective, wild-type allele and cells carrying the risk allele; however, costimulation with CD226 and CD3 caused CD4$^+$CD45RA$^-$ T cells harboring the risk allele to produce significantly more IL-17 than cells harboring the protective wild-type allele. Intracellular staining further demonstrated that populations of CD4$^+$ T cells harboring the risk allele showed a significant increase in the numbers of IL-17$^+$ IFN-γ$^-$ and IL-17$^+$ IFN-γ$^+$ CD4$^+$ T cells upon costimulation with CD3 and CD226 monoclonal antibodies (Fig. 6B). Consistent with our earlier experiments on signal transduction downstream of CD226-CD3 coactivation (Fig. 4), the enhanced IL-17 production resulting from co-engagement of CD3 and CD226 was associated with increased phosphorylation of ERK and VAV1, whereas it had no significant impact on AKT phosphorylation (Fig. 6C). To directly establish that the CD226 SNP causing the G307S substitution increased VAV1 activation, we expressed comparable amounts of CD226 harboring either the protective or the risk allele in Jurkat cells (Fig. 6D). Upon CD226 engagement, expression of the risk variant Ser^{307} led to greater phosphorylation of VAV1 as compared to expression of the Gly^{307} protective variant (Fig. 6D). These data therefore suggest that the VAV1-dependent cross-talk between CD3 and CD226 identified in this study is functionally relevant and likely contributes to the etiology of autoimmune diseases.

DISCUSSION

We combined mouse genetics with AP-MS to determine the VAV1 interactome in primary mouse CD4$^+$ T cells with a high degree of resolution. Primary CD4$^+$ T cells were stimulated with pervanadate, a potent inhibitor of tyrosine phosphatases. It is arguably not the most physiological way of stimulating T cells, but it is the best way to achieve maximal T cell activation of protein tyrosine kinases and optimize the identification of potential VAV1 interactors that should be further validated using classical biochemical approaches and functional assays. In support of such an approach, a previous study based on AP-MS analysis of endogenous signaling complexes in primary T cells and comparing the SLP76 interactome after T cell activation through the TCR or pervanadate showed that there was extensive overlap (74%) in the composition of protein complexes that assembled around SLP76-OST after pervanadate treatment or after activation of the TCR with CD3 and CD4 antibodies (*16*). We showed that the VAV1 interactome includes 50 partners, and we determined the kinetics of each protein binding to VAV1 during 300 s of T cell stimulation with pervanadate. We identified several previously unknown VAV1 partners, some of which have been identified as components of the LAT, SLP76, or ZAP70 signalosomes (*16*) using a similar approach. UBASH3A (ubiquitin-associated and SH3 domain–containing protein A), a tyrosine phosphatase that reduces TCR signaling through ZAP70 inactivation and TCR endocytosis, is the only protein, together with GRB2, that is consistently found in the VAV1, LAT, SLP76, and ZAP70 interactomes. Some of the VAV1-binding partners we identified are nuclear proteins (such as NF-κB1 and AIP), a finding congruent with previous reports demonstrating that VAV1 translocates into the nucleus and is found in transcriptionally active complexes (*30*). We also detected several VAV1 partners involved in cytoskeleton remodeling (WASP, WIPF1, ITK, and DBNL). In this regard, T cells from *Vav-1*$^{-/-}$ mice are defective in TCR-induced actin polymerization and at forming antigen-specific conjugates with antigen-presenting cells (APC) (*31*, *32*). Although mice deficient for ITK share similar T cell defects with mice

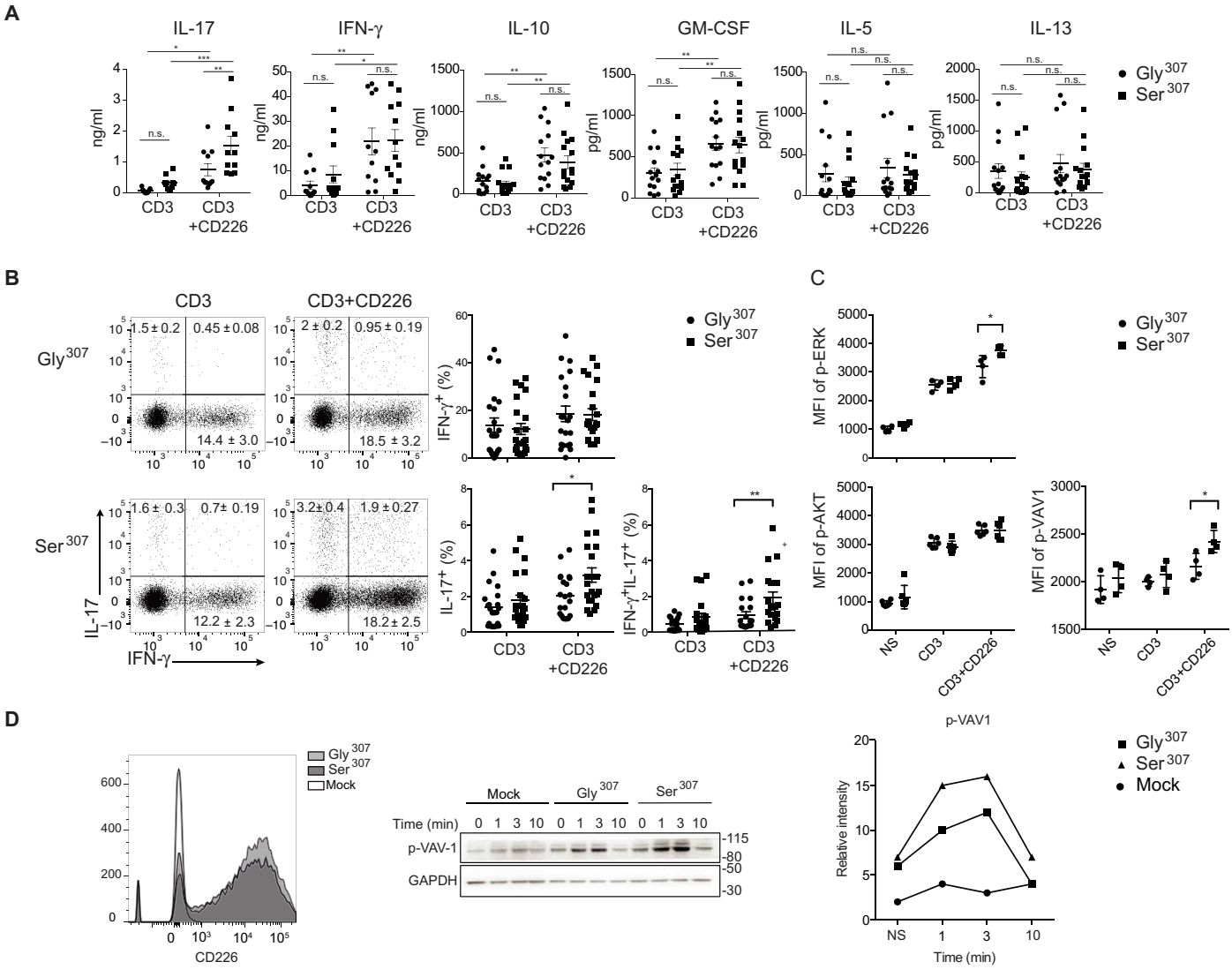

Fig. 6. The CD226 G307S variant enhances CD226-driven IL-17 production and VAV1 activation. (**A**) Cytokine secretion was quantified in supernatants of primary human $CD4^+CD45RA^-$ T cells expressing the Gly^{307} or the Ser^{307} variants of CD226, using enzyme-linked immunosorbent assays for IL-17 and IFN-γ (11 donors) or cytometric beads array assays for IL-5, IL-10, IL-13, and GM-CSF (14 donors). Cells were stimulated with antibodies that cross-link CD3 and CD226 molecules (CD3+CD226) or antibodies that cross-link only CD3 molecules (CD3) for 5 days. (**B**) Representative flow cytometry analysis of cells stained to show intracellular IL-17 and IFN-γ in primary human $CD4^+CD45RA^-$ T cells expressing the Gly^{307} or the Ser^{307} variants of CD226. Cells were stimulated as indicated in (A). The graphs summarize the data obtained from 20 unrelated donors. (**C**) Phosphoflow analysis of ERK, AKT, and VAV1 phosphorylation (p-ERK, p-AKT, and p-VAV1) in $CD4^+$ T cells that were unstimulated (NS) or stimulated with antibodies that cross-link CD3 and CD226 molecules (CD3+CD226) or antibodies that cross-link only CD3 molecules (CD3). Graphs represent data from four individual donors per genotype and are representative of three independent experiments. (**D**) Jurkat cells expressing the indicated CD226 variants or an empty vector (Mock) were stimulated by antibodies that cross-link the CD226 molecules for the indicated times, and the amount of p-VAV1 was determined by Western blot analysis. The graph shows the relative abundance of p-VAV1, determined as a ratio of the intensity of p-VAV1 to that of GAPDH during the time course of the experiment. The histogram shows the amount of CD226 Gly^{307} and CD226 Ser^{307} on the transfected Jurkat cells and are representative of two independent experiments. $^*P \leq 0.05$, $^{**}P \leq 0.01$, $^{***}P \leq 0.001$; n.s., not significant.

lacking WASP family proteins, these phenotypes do not completely overlap, consistent with the view that VAV1 is an essential element for nucleating all these effectors to trigger activation of downstream biological processes that depend on actin polymerization (*33*).

Because of the novelty and clinical relevance of the CD226-VAV1 interaction, the present study focused on that specific interaction and determined the mechanisms whereby CD226 promotes $CD4^+$ T cell activation. We focused our study on human T cells because of the quality of the reagents commercially available to probe human CD226 and their direct clinical relevance. Using monoclonal antibodies that act as agonists of CD226, we confirmed that VAV1 interacted with CD226 in Jurkat cells and in primary human $CD4^+$ T cells upon CD226 engagement. We showed that the engagement of CD226 mediated intrinsic signals in Jurkat cells, resulting in the activation of ERK and VAV1, two positive regulators of T cell activation. Protein kinase C and the Src kinase FYN have been postulated to phosphorylate CD226 (*34*–*36*) and thus are potential candidates for recruiting and subsequently activating VAV1. Experiments

aiming at inactivating those kinases in a separate or combined manner will be needed to formally address their respective contributions. We also observed that VAV1 was critical for CD226-driven ERK activation but dispensable for AKT signaling, demonstrating the importance of VAV1 for some, but not all, CD226 signaling pathways. We also revealed that CD226 synergized with the TCR-CD3 complex for optimal activation of both Jurkat cells and human primary $CD4^+$ T cells. Whether CD226 and TCR-CD3 trigger independent signaling pathways with common downstream outputs or whether CD226 and TCR signals are integrated through some TCR-dependent plasma membrane proximal hubs such as SLP76 is an important issue that remains to be addressed. Our observation that cross-linking (activation) of CD226 alone was not sufficient to trigger detectable intracellular signaling and proliferation in primary $CD4^+$ T cells suggests that CD226 does not act in an autonomous manner but synergizes with coincident signals elicited by the TCR-CD3 complex. Related to this, we would like to stress that a similar issue was raised for CD28 and the TCR-CD3 more than 20 years ago and remains heavily debated. Previous investigations done in NK cells have suggested that the adaptor protein SLP76 integrates signals elicited by distinct natural cytotoxicity receptors (NCRs), with full-blown activation only occurring when the various tyrosine residues present in SLP76 are selectively phosphorylated by inputs provided by different NCRs (*37*). Along the same line, a study using NK cells demonstrated that CD226 recruits VAV1, PI3K, and PLC-γ in a manner that depends on GRB2, leading to ERK, AKT, and Ca^{2+} signaling (*38*). However, our studies of the GRB2 and SLP76 interactomes in primary $CD4^+$ T cells failed to detect any interaction between CD226 and either GRB2 or SLP76 (*16*, *39*). Therefore, in contrast to the situation observed in NK cells, our results suggest that the recruitment of VAV1 to CD226 occurs in a manner that is independent of GRB2 and SLP76.

The involvement of CD226 in the production of cytokines by immune cells has been mostly studied in NK and $CD8^+$ T cells. $CD226^+CD8^+$ T cells have been shown to produce more IL-4, IL-5, IL-13, and IFN-γ than their CD226-negative counterparts (*40*). In NK cells, CD226 triggers production of IFN-γ, IL-6, and GM-CSF (*38*, *41*). Increased production of CD226 in regulatory T cells has been associated with reduced suppressive activity and augmented production of effector cytokines, including IFN-γ, IL-10, IL-13, and IL-17A (*42*). These data are congruent with our present study, which shows that the co-engagement of CD226 and CD3 on effector $CD4^+$ T cells with agonist antibodies stimulates the cells to secrete inflammatory cytokines but has no effect on naïve $CD4^+CD45RA^+$ T cells. Our VAV1 knockdown experiments demonstrated that, among the CD226-induced cytokines, VAV1 inhibition specifically affected IL-17. This selective effect may be linked to the specific inhibition of ERK pathways in VAV1 knockdown T cells, because ERK inhibition leads to defective T helper 17 cell (T_H17) differentiation. Other studies have demonstrated that TCR-mediated ERK phosphorylation is crucial for T_H17, but not T_H1 and T_H2, polarization and that sustained ERK phosphorylation is a characteristic feature of memory T_H17 cells (*43*, *44*).

Although a genetic variant of CD226 (CD226 G307S) has been described to predispose to several autoimmune and inflammatory diseases (*10*, *11*), no functional studies regarding its mode of action in effector $CD4^+$ T cells have been published. Our data demonstrate that both IL-17 production and the frequency of $CD4^+$ T cells that express IL-17 or IFN-γ and IL-17 (IFN-γ^+IL-17^+) were increased in humans carrying the risk variant allele upon engaging both CD3 and CD226 and that this was associated with increased VAV1 activation. Markedly, the impact of this SNP was undetected when the cells were stimulated with antibodies that stimulate only CD3. Therefore, the synergistic signals resulting from co-engagement of the TCR and of the CD226 costimulatory molecule constitute an important checkpoint in the tuning of proinflammatory cytokine production under both physiological and pathological conditions. Consistent with our study, most IFN-γ–producing T cells and all IL-17^+ cells found in humans express CD226, whereas IL-13–producing cells do not (*45*). In addition, blockade of CD226 signaling decreases IFN-γ and IL-17 production, whereas IL-5 and IL-13 secretion remains unaffected. Therefore, the mode of action of CD226 uncovered in the present study provides a rationale for the importance of blocking CD226 in autoimmune diseases involving T_H1 and T_H17 cells.

CD226 recognizes CD155 and CD112, which are also ligands for the inhibitory receptors TIGIT and CD96. One of the concerns in elucidating the functions of CD226 using CD226-deficient T cells is that the loss of CD226 not only obliterates CD226-dependent signals but also makes CD226 ligands available for potential binding to the TIGIT and CD96 inhibitory receptors (*38*, *46*). Therefore, enhanced triggering of TIGIT and CD96, rather than loss of CD226-dependent signals, might explain functional changes in CD226-deficient immune cells. Our findings showing that the direct co-engagement of CD226 by agonist antibody markedly enhances signaling and cytokine production in human $CD4^+$ T cells formally establish that these functions constitute intrinsic activities of CD226.

In conclusion, we have identified the CD226 costimulatory molecule among the VAV1 interactors in primary mouse $CD4^+$ T cells. Considering that CD226 is associated with various pathological conditions such as autoimmunity (*47*, *48*), we characterized the CD226-VAV1 or CD226/VAV1 signaling axis in human $CD4^+$ T cells. We showed that VAV1 is essential for delivering some of the signals triggered by CD226, including those leading to IL-17 production. Therefore, understanding the mode of action of T cell costimulatory molecules such as CD226 provides a rational basis for using them as targets for the management of inflammatory diseases or tumors.

MATERIALS AND METHODS

Generation of $VAV1^{OST}$ knock-in mice

A 6.2-kb genomic fragment containing exons 26 and 27 of the *Vav1* gene was isolated from a bacterial artificial chromosome (BAC) clone (clone no. RP23-95O21; http://www.lifesciences.sourcebioscience.com) of C57BL/6J origin. An OST-(Stop)2*lox*P-tACE-CRE-PGK-gb2-*neo*^{r}-*lox*P cassette was introduced at the 3′ end of the *Vav1* coding sequence found in exon 27. Finally, the targeting construct was abutted to a cassette for the expression of thymidine kinase. JM8.F6 C57BL/6N embryonic stem (ES) cells were electroporated with the *Vav1*^{OST}-targeting vector. After selection in G418 and ganciclovir, ES cell clones were screened for proper homologous recombination by Southern blot or polymerase chain reaction (PCR) analysis. When tested on Sac I–digested genomic DNA, the 5′ single-copy probe used to identify proper recombination events hybridized to a 8.9-kb wild-type fragment and to a 6.1-kb recombinant fragment. When tested on Xba I–digested genomic DNA, the 3′ single-copy probe used to identify proper recombination events hybridized to a 11.3-kb wild-type fragment and to a 7.0-kb recombinant fragment. A *neo*^{r}-specific probe was used to ensure that adventitious nonhomologous recombination events had not occurred in the selected ES clones. Mutant ES cells were injected into

FVB blastocysts. Germline transmission led to the self-excision of the loxP-tACE-CRE-PGK-gb2-neo-loxP cassette in male germinal cells. Screening for proper deletion of the loxP-tACECRE-PGK-gb2-neo-loxP cassette and for the presence of the sequence coding for the OST was performed by PCR using the following pair of primers: sense 5′-CAAGAGGGGTCCAACCTGCTGTGAT-3′ and antisense 5′-GTTCATGGCCCCTCAACCCTGCTAG-3′. This pair of primers amplified a 185-bp band for the wild-type allele and a 375-bp band for the *Vav1*^{OST} allele.

For characterization of the *Vav1*^{OST} knock-in model, mice were numbered by the animal facility, and the experiments were conducted and analyzed blindly. Both male and female from 6 to 10 weeks old were used to conduct experiments. No randomization was performed.

Wild-type and *Vav1*^{OST} (B6-*Vav1*^{tm1Mal}) knock-in mice were maintained under specific pathogen-free conditions at the INSERM animal facility (Zootechnie US-006), which is accredited by the French Ministry of Agriculture to perform experiments on live mice (accreditation number A-31 55508). All experimental protocols were approved by the ministry-approved ethics committee (CEEA-122) and are in compliance with the French and European regulations on care and protection of laboratory animals.

Flow cytometry

The monoclonal antibodies used for flow cytometry were as follows: AF-405 anti-mouse CD4 (RM4-5), AF-700 anti-mouse CD8 (53-6.7), phycoerythrin (PE)–Cy5 anti-mouse TCR (H57-597), fluorescein isothiocyanate (FITC) anti-mouse CD19, APC anti-mouse CD44 (IM7), Percp Cy5.5 anti-mouse CD62L (MEL-14), and PE–anti-human CD226 (DX11). The fluorescent-conjugated antibodies were purchased from eBiosciences, BD Biosciences, and BioLegend. For staining cells for flow cytometry analysis, 10^6 cells were incubated with monoclonal antibodies for 20 min at 4°C. After washing with phosphate-buffered saline (PBS) containing 5% fetal calf serum (FCS), the biotin-labeled cells were incubated with streptavidin-coupled PC7 for 20 min at 4°C and washed twice with PBS/5% FCS. Data were collected on an LSR-II (BD Biosciences).

Calcium flux measurement

For calcium flux analysis, CD4$^+$ T cells were loaded at 37°C for 30 min with the fluorescent calcium indicator Indo-1 (Invitrogen) at 5 μM. The cells were then washed and stained for TCR and CD4. Cells were incubated with biotynilated anti-CD3 monoclonal antibody (0.5 μg/ml; 145-2C11) at 37°C for 30 s. Medium was then added, and baseline quantities were measured for 30 s, at which time streptavidin (30 μg/ml; Sigma-Aldrich) was added for cross-linking. Events were recorded for an additional 250 s. The relative concentration of Ca^{2+} was measured as the ratio between the Ca^{2+}-bound dye and the Ca^{2+}-free dye. Data were analyzed using FlowJo software.

Mouse CD4$^+$ T cell isolation and short-term expansion

CD4$^+$ T cells were purified from pooled lymph nodes and spleens using the Dynabeads Untouched Mouse CD4$^+$ T Cell Kit (Life Technologies). Purified CD4$^+$ T cells (purity >95%) were briefly expanded with plate-bound anti-CD3 (3 μg/ml; 145-2C11) and soluble anti-CD28 monoclonal antibodies (1 μg/ml; clone 37.51, both from Exbio). After 48 hours of culture, CD4$^+$ T cells were harvested and rested in the presence of IL-2 (10 U/ml) for 48 hours before stimulation. The culture medium was RPMI 1640 (Gibco Life Technologies Ltd.) containing 10% of FCS, sodium pyruvate, nonessential amino acids, L-glutamine, penicillin-streptomycin, and 2×10^{-5} M 2-β-mercaptoethanol.

Stimulation and lysis of CD4$^+$ T cells

A total of 100×10^6 short-term expanded CD4$^+$ T cells from C57BL/6 and *Vav1*^{OST} mice were left unstimulated or stimulated at 37°C with pervanadate. Pervanadate stock solution was prepared as previously described (*16*). Stimulation was performed for 30, 120, and 300 s and stopped by the addition of a twice-concentrated lysis buffer [2% *n*-dodecyl-β-maltoside, 10% glycerol, 100 mM tris (pH 7.5), 270 mM NaCl, and 1 mM EDTA (pH 8)] supplemented with protease and phosphatase inhibitors. After 10 min of incubation on ice, cell lysates were centrifuged at 20,000*g* for 5 min at 4°C. Postnuclear lysates were used for affinity purification or immunoblot analysis. Anti-VAV1 (C-14, Santa Cruz Biotechnology), anti–P-VAV1 (Tyr^{174}, Santa Cruz Biotechnology), antibody to phosphorylated tyrosine (4G10; Millipore), anti-LAT (06-807; Millipore), anti-GRB2 (C-23; Santa Cruz Biotechnology), anti–PLC-γ1 (1249; Santa Cruz Biotechnology), and anti-GAPDH (FL-335; Santa Cruz Biotechnology) were used for immunoblot analysis.

Affinity purification of protein complexes

Postnuclear lysates were incubated with prewashed Strep-Tactin Sepharose beads (IBA GmbH) for 1.5 hours at 4°C on a rotary wheel. Beads were washed two times with 1 ml of lysis buffer complemented with detergent and phosphatase inhibitors and three times with 1 ml of lysis buffer in the absence of detergent and protease-phosphatase inhibitors. Proteins were eluted from the Strep-Tactin Sepharose beads with 2.5 mM D-biotin–containing buffer. Samples were analyzed by nano-LC coupled to either an LTQ Orbitrap Velos mass spectrometer (Thermo Fisher Scientific) (for samples of biological replicates 1 to 3) or a Q-Exactive mass spectrometer (Thermo Fisher Scientific) (for samples of biological replicate 4).

Tandem MS analysis

After affinity purification, protein samples were partially air-dried in a SpeedVac concentrator and then reconstituted in 1× final Laemmli buffer containing 25 mM dithiothreitol and heated at 95°C for 5 min. Cysteines were alkylated for 30 min at room temperature by the addition of a solution of 90 mM iodoacetamide. Protein samples were loaded on a one-dimensional acrylamide gel (stacking 4%, separating 12%) and the electrophoresis was stopped as soon as the protein sample entered the separation gel. The gel was briefly stained with Coomassie blue (Instant Blue, Expedeon), and a single slice containing the whole sample was excised. The gel slice was washed twice with 100 mM ammonium bicarbonate and once with 100 mM ammonium bicarbonate-acetonitrile (1:1). Proteins were in-gel–digested using 0.6 μg of modified sequencing-grade trypsin (Promega) in 50 mM ammonium bicarbonate overnight at 37°C. The resulting peptides were extracted from the gel by one round of incubation (15 min, 37°C) in 50 mM ammonium bicarbonate and two rounds of incubation (15 min each, 37°C) in 10% formic acid–acetonitrile (1:1). The extracted fractions were pooled with the initial digestion supernatant and dried in a speed-vac. Peptides were further purified by C18 zip-tip (Millipore) and analyzed by nano-LC coupled to either an LTQ Orbitrap Velos mass spectrometer (Thermo Fisher Scientific) (for samples of biological replicates 1 to 3) or a Q-Exactive mass spectrometer (Thermo Fisher Scientific) (for samples of biological replicate 4). Five microliters of each sample was loaded

on a C-18 precolumn (300 μm inner diameter × 5 mm; Dionex) in a solvent made of 5% acetonitrile and 0.05% trifluoroacetic acid at a flow rate of 20 μl/min. After 5 min of desalting, the precolumn was switched online with the analytical C-18 column (75 μm inner diameter × 50 cm; Reprosil C18) equilibrated in 95% solvent A (5% acetonitrile, 0.2% formic acid) and 5% solvent B (80% acetonitrile, 0.2% formic acid). Peptides were eluted using a 5 to 50% gradient of solvent B over 105 min at a flow rate of 300 nl/min. The mass spectrometer was operated in a data-dependent acquisition mode with Xcalibur software. On the LTQ-Velos, survey MS scans were acquired in the Orbitrap on the 350 to 1800 m/z range with the resolution set at 60,000 and automatic gain control (AGC) target at 1×10^6 ions, the 20 most intense ions were selected for collision-induced dissociation, and MS/MS spectra were acquired in the linear trap with an AGC target at 5×10^3 ions, maximum fill time at 100 ms, and a dynamic exclusion of 60 s to prevent repetitive selection of the same peptide. On the Q-Exactive, survey MS scans were acquired on the 350 to 1500 m/z range with the resolution set at 70,000 and AGC target at 3×10^6 ions, the 10 most intense ions were selected for higher-energy C-trap dissociation, and MS/MS spectra were acquired in Orbitrap with an AGC target at 1×10^5 ions, maximum fill time at 100 ms, and a dynamic exclusion of 30 s. Triplicate or duplicate technical LC-MS measurements were performed for each sample.

Protein identification and quantification

Raw MS files were processed with MaxQuant software (version 1.5.2.8) for database search with the Andromeda search engine and quantitative analysis. Data were searched against *Mus musculus* entries in the Swiss-Prot protein database (release UniProtKB/Swiss-Prot 2015-04; 16,699 entries). Carbamidomethylation of cysteine was set as a fixed modification, whereas oxidation of methionine, protein N-terminal acetylation, and phosphorylation of serine, threonine, and tyrosine were set as variable modifications. Specificity of trypsin digestion was set for cleavage after K or R, and two missed trypsin cleavage sites were allowed. The precursor mass tolerance was set to 20 parts per million (ppm) for the first search and 4.5 ppm for the main Andromeda database search. The mass tolerance in MS/MS mode was set to 0.6 Da. Minimum peptide length was set to seven amino acids, and minimum number of unique peptides was set to one. Andromeda results were validated by the target-decoy approach using a reverse database at both a peptide and protein false discovery rate of 1%. For label-free relative quantification of the samples, the match between runs option of MaxQuant was enabled with a time window of 1 min to allow cross-assignment of MS features detected in the different runs.

Unspecific binding protein filter

To identify the most specific VAV1-binding partners, the intensity metric from the MaxQuant protein group.txt output (sum of peptide intensity values for each protein) was used to compare proteins identified in samples purified from $CD4^+$ T cells from $Vav1^{OST}$ and from wild-type (control) mice. Intensity values were $\log_2$-transformed, and normalization across the compared samples (four biological replicates including four time points for both $Vav1^{OST}$ and wild type, representing a total of 32 samples, each analyzed in either two or three MS replicate runs) was performed by adjusting the medians of the distribution of logarithmized protein intensities for all runs. The experimental design (time course, stimulated or nonstimulated status, number of biological and technical replicates, and time point conditions) and the assessment of biological and technical variability across all the MS analyses (before and after normalization of the data) are illustrated in fig. S2. For the 32 samples, an average intensity value was calculated for each protein from the intensity values of the two or three MS technical replicate runs when available. Missing protein intensity values were replaced by a constant low intensity value representing the noise, calculated independently for each sample as the lowest one percentile value of the distribution of protein intensities. To determine whether a given detected protein was specifically associated with the Vav1-OST bait, we compared the distribution (across all biological replicates and time points) of log-normalized intensities obtained for 16 $Vav1^{OST}$ samples and for the 16 corresponding wild-type $CD4^+$ T cell samples. The comparison yielded a mean fold-change value specifying the global enrichment observed in $Vav1^{OST}$ T cells as compared to wild-type $CD4^+$ T cells and a corresponding P value based on a nonparametric Mann-Whitney test (volcano plot shown in Fig. 2A). This P value was corrected for multiple testing by BH adjustment. Proteins with a BH-adjusted $P <$ 0.05 and a fold change > 5 were reported as most confident VAV1-interacting proteins. To illustrate the evolution of the interactome across the kinetics of activation, a separate statistical analysis was performed by comparing the $Vav1^{OST}$ and wild-type samples at each time point (fig. S3C).

Kinetics of the binding of proteins to VAV1

Before analyzing the kinetics of assembly and disassembly of the proteins interacting with the VAV1 bait over 300 s of stimulation, the variability that may occur during affinity purification (yielding slightly distinct amounts of bait per sample) was corrected in each sample by normalizing the log-transformed, averaged protein intensity values through adjustment of the VAV1 bait intensity across the 32 samples. After this normalization step, missing protein intensity values were imputed with a noise value as described above. To facilitate the comparison of the kinetics of binding of different proteins with VAV1, protein intensity values were standardized on a 0-to-1 scale, with 1 corresponding to the highest value reached over the 300 s of stimulation. For each time point, SD across the four biological replicates was calculated, and proteins with a low mean SD value (mean SD across the four stimulation time points ≤ 0.25) were selected as VAV1-interacting proteins showing reproducible kinetics of interaction.

Human cell lines and primary $CD4^+$ T cells

The Jurkat E6.1 T cell line and its CD226-overexpressing variant were provided by R. Thorne (Cancer Research Unit, School of Biomedical Sciences, The University of Newcastle). Cells were grown in complete RPMI medium supplemented with normocin (100 μg/ml; Invivogen) to avoid bacterial, fungal, and mycoplasma contamination. Peripheral blood mononuclear leucocytes (PBMCs) were obtained from buffy coat preparations drawn from consenting anonymous healthy blood donors at the Purpan University Hospital blood bank (Toulouse, France). PBMCs were prepared by gradient centrifugation (MLS-Ficoll, Eurobio) of buffy coats. Monocytes were removed by plastic adherence, and $CD4^+$ T cells were purified by negative selection using $CD4^+$ T negative isolation kits (Dynabeads Untouched Human $CD4^+$ T Cell Kit, Life Technologies). The percentage of residual $CD8^+$ T cells after depletion was always less than 0.5%, and the remaining population consisted of 95 to 98% $CD4^+$ T cells and 2 to 5% $CD4^+$ $CD8^+$ double-negative non–T cells.

Enriched human $CD4^+$ T cells were sorted by flow cytometry into $CD4^+CD45RA^+$ naïve T cells and $CD4^+CD45RA^-$ effector/memory T cells (FACSAria; BD Biosciences). The purity of these subsets was higher than 98%. Local ethics committee approved our experimental protocols (N°DC-2015-2488).

SNP genotyping

We genotyped the presence of the CD226 SNP rs763361 by using the TaqMan SNP Genotyping Assay (Applied Biosystems) according to the manufacturer's protocols. Carriers of rs763361T allele were considered at risk, whereas rs763361C was termed protective allele. Experiments were done on cells from donors homozygous for each allele.

Plasmid construction

CD226 Gly^{307} plasmid was purchased from Origene. CD226 Ser^{307} plasmid was obtained by mutation using the QuikChange Lightning Site-Directed Mutagenesis Kit according to the manufacturer's recommendations (Agilent Technologies). Primers used from the mutagenesis are as follows: 5′-GTCCCATCTCTACCAGCCAACCTACCAATCAATCC-3′ (forward) and 5′-GGATTGATTGGTAGGTTGGCTGGTAGAGATGGGAC-3′ (reverse).

T cell electroporation

For Jurkat cell lines, 2×10^6 cells were mixed with 250 pmol of scrambled or VAV1 siRNA in Ingenio electroporated buffer (Mirus) and electroporated using the H-10 program of an Amaxa device (Lonza). The same program was used for the electroporation of CD226 plasmids. Before electroporation, primary $CD4^+$ T cells were briefly activated using plate-bound anti-CD3 (4 μg/ml; UCHT-1) and soluble anti-CD28 (1 μg/ml; CD28.2) in IL-2–containing medium (30 U/ml). After 48 hours of activation, cells were harvested and allowed to rest for 24 hours in complete medium. Cells (4×10^6) were then mixed with 250 pmol of scramble or VAV1 siRNA in Ingenio electroporated buffer (Mirus) and electroporated using the T-23 program of an Amaxa device (Lonza). Maximum VAV1 knockdown was achieved 72 hours after electroporation. Scramble siRNA (5′-AUUGUAUGCGAUCGCAGACdTdT-3′ and 5′-GUCUGCGAUCGCAUACAAUdTdT-3′) and VAV1 siRNA (5′-CGUCGAGGUCAAGCACAUUdTdT-3′ and 5′-AAUGUGCUUGACCUCGACGdTdT-3′) were purchased from Sigma-Aldrich.

Cell stimulation and immunoblot analysis

Jurkat cells and primary human $CD4^+$ T cells were stimulated with either anti-CD3 (UCHT-1) monoclonal antibody, anti-CD226 monoclonal antibody (NewE1, Millipore), or a combination of both. Cells were incubated with indicated antibodies for 30 min in ice, then washed with ice-cold free medium, resuspended in warm free medium (40×10^6 cells/ml), and left for 5 min at 37°C. Antibodies were cross-linked using goat anti-mouse Fab2 secondary antibody (20 μg/ml; Jackson ImmunoResearch) for the indicated times. Stimulation was stopped with addition of 2× lysis buffer (2% Triton X-100, phosphatase inhibitors). Activation of ERK1/2 and AKT was assessed by immunoblots with phospho-specific antibodies to ERK1/2 phosphorylated at Thr^{202} and Tyr^{204}, and to AKT phosphorylated at Ser^{473} (Cell Signaling Technology). CD226 was immunoblotted using DX11 antibody (BD Biosciences). Signals were detected with a ChemiDoc XRS system (Bio-Rad) and analyzed using the manufacturer's software.

Phosphoflow analysis

PBMCs for healthy donors were stimulated with anti-CD3 (UCHT-1) and anti-CD226 (NewE1) as previously described. Reaction was stopped and cells were permeabilized using a BD phosflow kit and Perm buffer III (BD Biosciences). Cells were stained using PE mouse-anti human p-ERK (pT202/pY204, clone 20A) and APC mouse anti-human p-Akt (pS473). For p-VAV1, cells were stained with unconjugated anti–p-VAV1 and then with an FITC anti-rabbit total IgG (Invitrogen). Samples were acquired on a Fortessa flow cytometer (BD Biosciences), and FlowJo software (TreeStar) was used for data analysis.

VAV1 immunoprecipitation

For VAV1 immunoprecipitation, Jurkat cells or primary $CD4^+$ T cell suspensions were stimulated using anti-CD226 antibody (NewE1, Millipore). Stimulation was stopped by the addition of twice-concentrated lysis buffer [100 mM tris (pH 7.5), 270 mM NaCl, 1 mM EDTA, 20% glycerol, and 0.2% *n*-dodecyl-β-maltoside] containing protease and phosphatase inhibitors. After 10 min of incubation on ice, cell lysates were centrifuged at 20,000*g* for 5 min at 4°C. Immunoprecipitations were performed using the VAV1 C14 antibody (Santa Cruz Biotechnology) or anti–p-VAV1 antibody (Tyr^{174}) and Prot-G Sepharose beads (Santa Cruz Biotechnology). After washing, proteins were eluted with Laemmli buffer and analyzed by SDS–polyacrylamide gel electrophoresis followed by Western blotting on polyvinylidene difluoride membranes (Immobilon). ECL Prime (Amersham) was used as revelation substrate.

Analysis of cytokine production using multiplexed bead-based immunoassays

Human $CD4^+$ T cells (10^4 per well) were stimulated with plate-bound anti-CD3 (4 μg/ml), anti-CD226, (clone NewE1; Millipore) at 5 or 10 μg/ml, and/or LEAF-purified mouse IgG1 isotype control (BioLegend). Cytokine secretion was assessed after 3 to 5 days of culture using Multiplexed Bead-Based Immunoassays (BD Biosciences) following the manufacturer's instructions.

Intracellular cytokine staining

Before detection of intracellular cytokine production, T cells were restimulated with phorbol 12-myristate 13-acetate (50 ng/ml) plus ionomycin (250 ng/ml) for 4 hours in the presence of GolgiStop (BD Biosciences). Staining with the LIVE/DEAD Fixable Dead Cell Stain Kit (Molecular Probes) was performed before fixation to allow gating on viable cells. After fixation and permeabilization with Staining Buffer (eBioscience), cells were stained with FITC anti–IFN-γ (B27) and APC anti–IL-17 (BL168) (BioLegend). Samples were acquired on a Fortessa flow cytometer (BD Biosciences), and FlowJo software (TreeStar) was used for data analysis.

Statistical analysis

Sample sizes were chosen based on previous experience in our laboratory. Statistical analyses, including sample variances in each group, were performed in GraphPad Prism version 6.0 software. Statistical significance was determined by *t* tests (two-tailed; $*P < 0.05$, $**P < 0.01$, $***P < 0.001$). Results are presented as means ± SEM, unless stated otherwise. No data were excluded from the statistical analysis.

SUPPLEMENTARY MATERIALS

www.sciencesignaling.org/cgi/content/full/11/538/eaar3083/DC1

Fig. S1. Structure of the 3′ end of the wild-type *VAV1* allele and the $VAV1^{OST}$ allele.

Fig. S2. Assessment of biological and technical variability across samples.
Fig. S3. The VAV1 interactome.
Fig. S4. The synergistic effect of CD3 and CD226 co-engagement is not observed in naïve $CD4^+$ T cells.
Table S1. List of proteins associated with VAV1 in resting and pervanadate-activated $CD4^+$ T cells.

REFERENCES AND NOTES

1. V. L. J. Tybulewicz, Vav-family proteins in T-cell signalling. *Curr. Opin. Immunol.* **17**, 267–274 (2005).
2. S. Katzav, D. Martin-Zanca, M. Barbacid, vav, a novel human oncogene derived from a locus ubiquitously expressed in hematopoietic cells. *EMBO J.* **8**, 2283–2290 (1989).
3. S. Kassem, G. Gaud, I. Bernard, M. Benamar, A. S. Dejean, R. Liblau, G. J. Fournié, C. Colacios, B. Malissen, A. Saoudi, A natural variant of the T cell receptor-signaling molecule Vav1 reduces both effector T cell functions and susceptibility to neuroinflammation. *PLOS Genet.* **12**, e1006185 (2016).
4. A. Saveliev, L. Vanes, O. Ksionda, J. Rapley, S. J. Smerdon, K. Rittinger, V. L. J. Tybulewicz, Function of the nucleotide exchange activity of Vav1 in T cell development and activation. *Sci. Signal.* **2**, ra83 (2009).
5. A. Tarakhovsky, M. Turner, S. Schaal, P. J. Mee, L. P. Duddy, K. Rajewsky, V. L. J. Tybulewicz, Defective antigen receptor-mediated proliferation of B and T cells in the absence of Vav. *Nature* **374**, 467–470 (1995).
6. P. S. Costello, A. E. Walters, P. J. Mee, M. Turner, L. F. Reynolds, A. Prisco, N. Sarner, R. Zamoyska, V. L. J. Tybulewicz, The Rho-family GTP exchange factor Vav is a critical transducer of T cell receptor signals to the calcium, ERK, and NF-κB pathways. *Proc. Natl. Acad. Sci. U.S.A.* **96**, 3035–3040 (1999).
7. K.-D. Fischer, Y.-Y. Kong, H. Nishina, K. Tedford, L. E. Marengère, I. Kozieradzki, T. Sasaki, M. L. Starr, G. M. Chan, S. L. Gardener, M.-Q. Nghiem, D. A. Bouchard, M. Barbacid, A. M. Bernstein, J. M. Penninger, Vav is a regulator of cytoskeletal reorganization mediated by the T-cell receptor. *Curr. Biol.* **8**, 554–562 (1998).
8. L. F. Reynolds, L. A. Smyth, T. Norton, N. Freshney, J. Downward, D. Kioussis, V. L. J. Tybulewicz, Vav1 transduces T cell receptor signals to the activation of phospholipase C-γ1 via phosphoinositide 3-kinase-dependent and -independent pathways. *J. Exp. Med.* **195**, 1103–1114 (2002).
9. S. P. Hehner, T. G. Hofmann, O. Dienz, W. Dröge, M. L. Schmitz, Tyrosine-phosphorylated Vav1 as a point of integration for T-cell receptor- and CD28-mediated activation of JNK, p38, and interleukin-2 transcription. *J. Biol. Chem.* **275**, 18160–18171 (2000).
10. J. P. Hafler, L. M. Maier, J. D. Cooper, V. Plagnol, A. Hinks, M. J. Simmonds, H. E. Stevens, N. M. Walker, B. Healy, J. M. M. Howson, M. Maisuria, S. Duley, G. Coleman, S. C. L. Gough; International Multiple Sclerosis Genetics Consortium (IMSGC), J. Worthington, V. K. Kuchroo, L. S. Wicker, J. A. Todd, CD226 Gly307Ser association with multiple autoimmune diseases. *Genes Immun.* **10**, 5–10 (2009).
11. Z.-X. Qiu, K. Zhang, X.-S. Qiu, M. Zhou, W.-M. Li, CD226 Gly307Ser association with multiple autoimmune diseases: A meta-analysis. *Hum. Immunol.* **74**, 249–255 (2013).
12. M. R. Junttila, S. Saarinen, T. Schmidt, J. Kast, J. Westermarck, Single-step *Strep*-tag purification for the isolation and identification of protein complexes from mammalian cells. *Proteomics* **5**, 1199–1203 (2005).
13. P. E. Paz, S. Wang, H. Clarke, X. Lu, D. Stokoe, A. Abo, Mapping the Zap-70 phosphorylation sites on LAT (linker for activation of T cells) required for recruitment and activation of signalling proteins in T cells. *Biochem. J.* **356**, 461–471 (2001).
14. Z. S. Ye, D. Baltimore, Binding of Vav to Grb2 through dimerization of Src homology 3 domains. *Proc. Natl. Acad. Sci. U.S.A.* **91**, 12629–12633 (1994).
15. A. Braiman, M. Barda-Saad, C. L. Sommers, L. E. Samelson, Recruitment and activation of PLCγ1 in T cells: A new insight into old domains. *EMBO J.* **25**, 774–784 (2006).
16. R. Roncagalli, S. Hauri, F. Fiore, Y. Liang, Z. Chen, A. Sansoni, K. Kanduri, R. Joly, A. Malzac, H. Lähdesmaki, R. Lahesmaa, S. Yamasaki, T. Saito, M. Malissen, R. Aebersold, M. Gstaiger, B. Malissen, Quantitative proteomics analysis of signalosome dynamics in primary T cells identifies the surface receptor CD6 as a Lat adaptor-independent TCR signaling hub. *Nat. Immunol.* **15**, 384–392 (2014).
17. M. Barda-Saad, N. Shirasu, M. H. Pauker, N. Hassan, O. Perl, A. Balbo, H. Yamaguchi, J. C. D. Houtman, E. Appella, P. Schuck, L. E. Samelson, Cooperative interactions at the SLP-76 complex are critical for actin polymerization. *EMBO J.* **29**, 2315–2328 (2010).
18. N. J. Hassan, S. J. Simmonds, N. G. Clarkson, S. Hanrahan, M. J. Puklavec, M. Bomb, A. N. Barclay, M. H. Brown, CD6 regulates T-cell responses through activation-dependent recruitment of the positive regulator SLP-76. *Mol. Cell. Biol.* **26**, 6727–6738 (2006).
19. J. Wu, Q. Zhao, T. Kurosaki, A. Weiss, The Vav binding site (Y315) in ZAP-70 is critical for antigen receptor-mediated signal transduction. *J. Exp. Med.* **185**, 1877–1882 (1997).
20. F. Michel, L. Grimaud, L. Tuosto, O. Acuto, Fyn and ZAP-70 are required for Vav phosphorylation in T cells stimulated by antigen-presenting cells. *J. Biol. Chem.* **273**, 31932–31938 (1998).
21. M. López-Lago, H. Lee, C. Cruz, N. Movilla, X. R. Bustelo, Tyrosine phosphorylation mediates both activation and downmodulation of the biological activity of Vav. *Mol. Cell. Biol.* **20**, 1678–1691 (2000).
22. D. Dombroski, R. A. Houghtling, C. M. Labno, P. Precht, A. Takesono, N. J. Caplen, D. D. Billadeau, R. L. Wange, J. K. Burkhardt, P. L. Schwartzberg, Kinase-independent functions for Itk in TCR-induced regulation of Vav and the actin cytoskeleton. *J. Immunol.* **174**, 1385–1392 (2005).
23. E. Zvezdova, J. Mikolajczak, A. Garreau, M. Marcellin, L. Rigal, J. Lee, S. Choi, G. Blaize, J. Argenty, J. Familiades, L. Li, A. Gonzalez de Peredo, O. Burlet-Schiltz, P. E. Love, R. Lesourne, Themis1 enhances T cell receptor signaling during thymocyte development by promoting Vav1 activity and Grb2 stability. *Sci. Signal.* **9**, ra51 (2016).
24. W. Paster, C. Brockmeyer, G. Fu, P. C. Simister, B. de Wet, A. Martinez-Riaño, J. A. H. Hoerter, S. M. Feller, C. Wülfing, N. R. J. Gascoigne, O. Acuto, GRB2-mediated recruitment of THEMIS to LAT is essential for thymocyte development. *J. Immunol.* **190**, 3749–3756 (2013).
25. N. Ramesh, R. Geha, Recent advances in the biology of WASP and WIP. *Immunol. Res.* **44**, 99–111 (2009).
26. S. Le Bras, I. Foucault, A. Foussat, C. Brignone, O. Acuto, M. Deckert, Recruitment of the actin-binding protein HIP-55 to the immunological synapse regulates T cell receptor signaling and endocytosis. *J. Biol. Chem.* **279**, 15550–15560 (2004).
27. W. M. Henne, E. Boucrot, M. Meinecke, E. Evergren, Y. Vallis, R. Mittal, H. T. McMahon, FCHo proteins are nucleators of clathrin-mediated endocytosis. *Science* **328**, 1281–1284 (2010).
28. L. L. Dragone, L. A. Shaw, M. D. Myers, A. Weiss, SLAP, a regulator of immunoreceptor ubiquitination, signaling, and trafficking. *Immunol. Rev.* **232**, 218–228 (2009).
29. K. J. Ralston, S. L. Hird, X. Zhang, J. L. Scott, B. Jin, R. F. Thorne, M. C. Berndt, A. W. Boyd, G. F. Burns, The LFA-1-associated molecule PTA-1 (CD226) on T cells forms a dynamic molecular complex with protein 4.1G and human discs large. *J. Biol. Chem.* **279**, 33816–33828 (2004).
30. M. Houlard, R. Arudchandran, F. Regnier-Ricard, A. Germani, S. Gisselbrecht, U. Blank, J. Rivera, N. Varin-Blank, Vav1 is a component of transcriptionally active complexes. *J. Exp. Med.* **195**, 1115–1127 (2002).
31. C. Wülfing, A. Bauch, G. R. Crabtree, M. M. Davis, The vav exchange factor is an essential regulator in actin-dependent receptor translocation to the lymphocyte–antigen-presenting cell interface. *Proc. Natl. Acad. Sci. U.S.A.* **97**, 10150–10155 (2000).
32. M. Villalba, K. Bi, F. Rodriguez, Y. Tanaka, S. Schoenberger, A. Altman, Vav1/Rac-dependent actin cytoskeleton reorganization is required for lipid raft clustering in T cells. *J. Cell Biol.* **155**, 331–338 (2001).
33. A. V. Miletic, D. B. Graham, K. Sakata-Sogawa, M. Hiroshima, M. J. Hamann, S. Cemerski, T. Kloeppel, D. D. Billadeau, O. Kanagawa, M. Tokunaga, W. Swat, Vav links the T cell antigen receptor to the actin cytoskeleton and T cell activation independently of intrinsic guanine nucleotide exchange activity. *PLOS ONE* **4**, e6599 (2009).
34. J. Shirakawa, K. Shibuya, A. Shibuya, Requirement of the serine at residue 329 for lipid raft recruitment of DNAM-1 (CD226). *Int. Immunol.* **17**, 217–223 (2005).
35. K. Shibuya, J. Shirakawa, T. Kameyama, S.-i. Honda, S. Tahara-Hanaoka, A. Miyamoto, M. Onodera, T. Sumida, H. Nakauchi, H. Miyoshi, A. Shibuya, CD226 (DNAM-1) is involved in lymphocyte function–associated antigen 1 costimulatory signal for naive T cell differentiation and proliferation. *J. Exp. Med.* **198**, 1829–1839 (2003).
36. A. Shibuya, L. L. Lanier, J. H. Phillips, Protein kinase C is involved in the regulation of both signaling and adhesion mediated by DNAX accessory molecule-1 receptor. *J. Immunol.* **161**, 1671–1676 (1998).
37. H. S. Kim, E. O. Long, Complementary phosphorylation sites in the adaptor protein SLP-76 promote synergistic activation of natural killer cells. *Sci. Signal.* **5**, ra49 (2012).
38. Z. Zhang, N. Wu, Y. Lu, D. Davidson, M. Colonna, A. Veillette, DNAM-1 controls NK cell activation via an ITT-like motif. *J. Exp. Med.* **212**, 2165–2182 (2015).
39. E. Caron, R. Roncagalli, T. Hase, W. E. Wolski, M. Choi, M. G. Menoita, S. Durand, A. García-Blesa, I. Fierro-Monti, T. Sajic, M. Heusel, T. Weiss, M. Malissen, R. Schlapbach, B. C. Collins, S. Ghosh, H. Kitano, R. Aebersold, B. Malissen, M. Gstaiger, Precise temporal profiling of signaling complexes in primary cells using SWATH mass spectrometry. *Cell Rep.* **18**, 3219–3226 (2017).
40. M. Ayano, H. Tsukamoto, K. Kohno, N. Ueda, A. Tanaka, H. Mitoma, M. Akahoshi, Y. Arinobu, H. Niiro, T. Horiuchi, K. Akashi, Increased CD226 expression on $CD8^+$ T cells is associated with upregulated cytokine production and endothelial cell injury in patients with systemic sclerosis. *J. Immunol.* **195**, 892–900 (2015).
41. L. Martinet, L. Ferrari De Andrade, C. Guillerey, J. S. Lee, J. Liu, F. Souza-Fonseca-Guimaraes, D. S. Hutchinson, T. B. Kolesnik, S. E. Nicholson, N. D. Huntington, M. J. Smyth, DNAM-1 expression marks an alternative program of NK cell maturation. *Cell Rep.* **11**, 85–97 (2015).
42. C. A. Fuhrman, W.-I. Yeh, H. R. Seay, P. Saikumar Lakshmi, G. Chopra, L. Zhang, D. J. Perry, S. A. McClymont, M. Yadav, M.-C. Lopez, H. V. Baker, Y. Zhang, Y. Li, M. Whitley, D. von Schack, M. A. Atkinson, J. A. Bluestone, T. M. Brusko, Divergent phenotypes of

human regulatory T cells expressing the receptors TIGIT and CD226. *J. Immunol.* **195**, 145–155 (2015).
43. F. Mele, C. Basso, C. Leoni, D. Aschenbrenner, S. Becattini, D. Latorre, A. Lanzavecchia, F. Sallusto, S. Monticelli, ERK phosphorylation and miR-181a expression modulate activation of human memory T_H17 cells. *Nat. Commun.* **6**, 6431 (2015).
44. H. Liu, S. Yao, S. M. Dann, H. Qin, C. O. Elson, Y. Cong, ERK differentially regulates Th17- and Treg-cell development and contributes to the pathogenesis of colitis. *Eur. J. Immunol.* **43**, 1716–1726 (2013).
45. E. Lozano, N. Joller, Y. Cao, V. K. Kuchroo, D. A. Hafler, The CD226/CD155 interaction regulates the proinflammatory (Th1/Th17)/anti-inflammatory (Th2) balance in humans. *J. Immunol.* **191**, 3673–3680 (2013).
46. L. Martinet, M. J. Smyth, Balancing natural killer cell activation through paired receptors. *Nat. Rev. Immunol.* **15**, 243–254 (2015).
47. S. Gilfillan, C. J. Chan, M. Cella, N. M. Haynes, A. S. Rapaport, K. S. Boles, D. M. Andrews, M. J. Smyth, M. Colonna, DNAM-1 promotes activation of cytotoxic lymphocytes by nonprofessional antigen-presenting cells and tumors. *J. Exp. Med.* **205**, 2965–2973 (2008).
48. A. K. Maiti, X. Kim-Howard, P. Viswanathan, L. Guillén, X. Qian, A. Rojas-Villarraga, C. Sun, C. Cañas, G. J. Tobón, K. Matsuda, N. Shen, A. C. Cherñavsky, J.-M. Anaya, S. K. Nath, Non-synonymous variant (Gly307Ser) in CD226 is associated with susceptibility to multiple autoimmune diseases. *Rheumatology* **49**, 1239–1244 (2010).

Acknowledgments: We thank A. Dejean, D. Gonzalez-Dunia, R. Liblau, and R. Lesourne for their comments on the manuscript. We acknowledge the technical assistance provided by the personnel of INSERM US006 Anexplo/Creffre Animal Facility; F.-E. L'Faqihi, V. Duplan, and L. Iscache from the flow cytometry core facility of Centre de Physiopathologie Toulouse Purpan (CPTP); and R. Romieu-Mourez and P.-E. Paulet from the CPTP immunomonitoring platform for the PBMC biobank. We thank A.-M. Mura and B. Estèbe [Centre d'Immunophénomique (CIPHE)] for the construction of the *Vav1*^{OST} mice and M. Michieletto for the generation of the CD226 Ser^{307} plasmid. **Funding**: This work was supported by INSERM (to A.S. and B. Malissen), Fondation pour la Recherche Médicale (DEQ2000326531 and DEQ20170336727 to A.S.), Association Française contre les Myopathies (to A.S.), Agence Nationale de la Recherche (ANR-08-GENO-041-01 to A.S.), Association de Recherche sur la Sclérose En Plaques (to A.S.), Région Midi-Pyrénées (to A.S. and B. Monsarrat), Fight-MG (FP7-Health-2009-242210 to A.S.), the French Ministry of Research with the Investissement d'Avenir Infrastructures Nationales en Biologie et Santé program (Proteomics French Infrastructure, ANR-10-INBS-08 to B. Monsarrat and O.B.-S.), PHENOMIN (French National Infrastructure for mouse Phenogenomics; ANR10-INBS-07 to B. Malissen), and European Research Council [FP7/2007-2013 grant no. 322465 ("Integrate") to B. Malissen]. A.S., A.G.d.P., O.B.-S., R.R., and B. Malissen were supported by Centre National de la Recherche Scientifique, and I.B. was supported by INSERM. **Author contributions**: A.S. and B. Malissen conceived the project. G.G., R.R., A.G.d.P., B. Monsarrat, O.B.-S., and A.S. conceived and designed the experiments. G.G., R.R., J.F., S.K., I.B., C.C., and K.C. performed the experiments. B. Malissen and R.R. supervised the construction and validation of the *Vav1*^{OST} knock-in mice. G.G., R.R., A.G.d.P., and K.C. analyzed the data. G.G., B. Malissen, A.G.d.P., R.R., and A.S. wrote the paper. **Competing interests:** The authors declare that they have no competing financial interests. **Data and materials availability:** All raw MS files, as well as protein identification and quantitative results from the MaxQuant software, have been deposited to the ProteomeXchange Consortium via the PRoteomics IDEntifications (PRIDE) partner repository with the data set identifier PXD004217.

Submitted 24 October 2017
Accepted 6 June 2018
Published 10 July 2018
10.1126/scisignal.aar3083

Citation: G. Gaud, R. Roncagalli, K. Chaoui, I. Bernard, J. Familiades, C. Colacios, S. Kassem, B. Monsarrat, O. Burlet-Schiltz, A. G. de Peredo, B. Malissen, A. Saoudi, The costimulatory molecule CD226 signals through VAV1 to amplify TCR signals and promote IL-17 production by $CD4^+$ T cells. *Sci. Signal.* **11**, eaar3083 (2018).

Science Signaling

The costimulatory molecule CD226 signals through VAV1 to amplify TCR signals and promote IL-17 production by CD4 $^{+}$ T cells

Guillaume Gaud, Romain Roncagalli, Karima Chaoui, Isabelle Bernard, Julien Familiades, Céline Colacios, Sahar Kassem, Bernard Monsarrat, Odile Burlet-Schiltz, Anne Gonzalez de Peredo, Bernard Malissen and Abdelhadi Saoudi

Sci. Signal. **11** (538), eaar3083.
DOI: 10.1126/scisignal.aar3083originally published online July 10, 2018

VAV1, a T cell hub

The guanine nucleotide exchange factor VAV1 is required for T cell receptor (TCR) signaling and activation of T cells. By analyzing the VAV1 interactome, Gaud *et al*. found that VAV1 also interacted with the costimulatory molecule CD226. Engagement of CD226 activated VAV1, which in turn enhanced the TCR-dependent production of the proinflammatory cytokine IL-17 by human T cells. A variant of CD226 that is associated with autoimmune diseases stimulated more VAV1 activity and IL-17 production than did wild-type CD226, demonstrating that VAV1-mediated cross-talk between the CD226 and TCR signaling pathways affects both normal and pathological T cell activation.